International Journal of Mechanical, Industrial and Aerospace Sciences
ISSN: 2517-9950
Vol:11, No:1, 2017

Frictional Effects on the Dynamics of a Truncated Double-Cone Gravitational Motor

Barenten Suciu

***Abstract*—**In this work, effects of the friction and truncation on the dynamics of a double-cone gravitational motor, self-propelled on a straight V-shaped horizontal rail, are evaluated. Such mechanism has a variable radius of contact, and, on one hand, it is similar to a pulley mechanism that changes the potential energy into the kinetic energy of rotation, but on the other hand, it is similar to a pendulum mechanism that converts the potential energy of the suspended body into the kinetic energy of translation along a circular path. Movies of the self-propelled double-cones, made of S45C carbon steel and wood, along rails made of aluminum alloy, were shot for various opening angles of the rails. Kinematical features of the double-cones were estimated through the slow-motion processing of the recorded movies. Then, a kinematical model is derived under assumption that the distance traveled by the contact points on the rectilinear rails is identical with the distance traveled by the contact points on the truncated conical surface. Additionally, a dynamic model, for this particular contact problem, was proposed and validated against the experimental results. Based on such model, the traction force and the traction torque acting on the double-cone are identified. One proved that the rolling traction force is always smaller than the sliding friction force; i.e., the double-cone is rolling without slipping. Results obtained in this work can be used to achieve the proper design of such gravitational motor.

***Keywords*—**Truncated double-cone, friction, rolling and sliding, dynamic model, gravitational motor.

I. Introduction

SKETCHES of Leonardo da Vinci are often mentioned in connection with the "over-balanced wheel" and "ascending (double)-cone" [1], [2], which are both gravitational motors able to convert the inputted potential energy into the outputted rotational and/or translational kinetic energy. Such motors can operate by harnessing energy from the gravitational field of the Earth, i.e. from an environmentally friendly source of energy. In 1829, the concept of a self-propelled railway vehicle was proposed, and although it was not materialized, it can be seen as a commendable attempt to turn into practice the double-cone gravitational motor. Such vehicle was imagined as having a central "body" with conical "wheels" applied at its ends, and running on three-dimensionally curved rails [3]. Obviously, such gravitational train could not compete with trains using combustible and electrical energy sources. Still, nowadays trains employ slightly conical wheels, to reduce the rubbing and to ease the movement of the vehicle around curves [4].

Double-cone gravitational motor might have applicative potential as generator of electrical power, but in order to cause the expediency of its industrial production, the concrete range of practical applications should be decided according to its range for the efficiency and outputted power. In order to design appropriately such gravitational motor, an unsophisticated but accurate theoretical model is required. Apparent paradox of the ascending double-cone is presented in the Physics classroom in correlation with the center of gravity and the moment of inertia, through facile tests and simplified theoretical models [5]. Also, complex mathematical and physical models, dedicated to cones traveling on rectilinear rails, horizontally or upwardly directed [6], or addressing sophisticated problems related to the rolling friction of various bodies of revolution [7], were reported.

Recently, a simple geometrical and kinematical model associated to double-cones, traveling on straight V-shaped horizontally displaced rails, was proposed [8]. Such analysis revealed that the points of contact between the double-cone and rails move on the conical surface along a logarithmic spiral. Based on common geometrical conditions, the maximal number of rotations, to be achieved by the double-cone, was estimated [8]. Such model predicted a slightly larger number of rotations, with a maximal relative error of 10-20 %, for carbon steel double-cones traveling along aluminum rails. However, the model accuracy, for double-cones and rails made of different materials, was not evaluated.

For this reason, in the present work, films of double-cones made of S45C carbon steel and Japanese beech, self-propelling on horizontal V-shaped rails, made of aluminum alloy, are shot for different entrance spans of the rails. Then, the previously suggested kinematical model [8] is improved to achieve higher accuracy, by including the effect of cone truncation. Our target is to achieve theoretical predictions with a relative error lower than 5%, relative to the number of rotations determined from the slow-motion analysis of the taken films.

Supplementarily, a model based on the Laws of Dynamics, applied for both motions of rotation and translation of the double-cone, is proposed and then, validated relative to the total traveling time determined from the rolling tests. This model allows for a thorough evaluation of the dynamic characteristics of the conical gravitational motor. For instance, the traction force and the traction torque acting on the double-cone can be clarified, and the self-propelling ability can be interpreted based on the movement regime of rolling without slipping.

II. Test Rig and Experimental Procedure

Two cones, made of the same material, each having a height of $H = 100$ mm, and a radius at the base circle of $R = 25$ mm, are joined together by using a bonding adhesive, to achieve the so-called double-cone (Fig. 1). Therefore, the apex angle of the cone can be calculated as: $\Psi = \tan^{-1}(R/H) = 14.036$ deg (see

Barenten Suciu is with the Department of Intelligent Mechanical Engineering, Fukuoka Institute of Technology, Fukuoka, 811-0295 Japan (phone: +81-92-606-4348; fax: +81-92-606-0747; e-mail: suciu@fit.ac.jp).

Fig. 2). However, the actual manufactured cones are slightly truncated, to avoid eventual injuries by the needle-like conical tips (see section IV for the geometrical details).

Two double-cones, one made of S45C carbon steel and the other made in wood (Japanese beech), were fabricated. Material diversity helps in our quest to clarify the influence of the rolling and sliding on the dynamics of the conical gravitational motor.

Table I shows, for the geometrically idealized double-cones, the physical properties (i.e., the diameter $2R$ of the base circle, the total height $2H$, the apex angle Ψ, the mass m, and the moment of inertia $I = 0.3mR^2$); then, the material properties (i.e., the modulus of elasticity E_c, and the Poisson's ratio v_c); and finally, the tribological properties (i.e., the static and dynamic friction coefficients μ_s and μ, given for parts from steel or wood, sliding on a counter-part made of aluminum alloy [9]-[11]). Rails have the modulus of elasticity of E_r = 74 GPa, the Poisson's ratio of $v_r = 0.33$, the length of $L_0 = 1{,}000$ mm (Fig. 2), the height of $H_0 = 50$ mm (Fig. 8), and the chamfering radius of $R_0 = 1$ mm (Fig. 8). They are disposed on a horizontal table to form a V letter, which has an entrance span L_2 and an exit span L_1, where $L_2 \leq L_1$ (see Fig. 2).

TABLE I
PHYSICAL, MATERIAL, AND TRIBOLOGICAL PROPERTIES OF THE GEOMETRICALLY IDEALIZED DOUBLE-CONES MADE OF STEEL AND WOOD

Property	Metallic double-cone	Wooden double-cone
Diameter, $2R$ [mm]	50	50
Total height (length), $2H$ [mm]	200	200
Apex angle, Ψ [deg]	14.036	14.036
Mass, m [kg]	1.051	0.1102
Moment of inertia, I [kg·mm^2]	197.0625	20.6625
Material	S45C carbon steel	Japanese beech
Modulus of elasticity, E_c [GPa]	206	13
Poisson's ratio, v_c [-]	0.3	0.35
Static friction coefficient, μ_s [-]	0.61	0.3
Dynamic friction coefficient, μ [-]	0.47	0.2

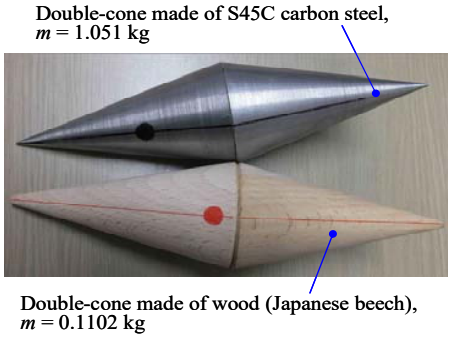

Fig. 1 Photographs of the tested metallic and wooden double-cones

Fig. 2 illustrates a schematic view of the metallic or wooden double-cone, rolling on the V-shaped horizontal rails. Exit span of the tracks is set to a constant value of L_1 = 185 mm. On the other hand, the entrance span L_2 of the rails is taken as variable, i.e., it is adjusted, starting from L_2 = 0 mm, with a pitch of 10 mm (see Table II). For instance, Fig. 3 illustrates photographs of the metallic and wooden double-cones for an entrance span of L_2 = 0 mm. Note that for $L_2 = L_1$, tracks become parallel, and in such case, the double-cone is unable to self-propel along the rails. Influence of the entrance span is quantified by defining an opening angle $\Phi = \sin^{-1}(0.5(L_1 - L_2)/L_0)$ of the rails (Fig. 2).

One proved that the opening angle decreases almost linearly from its maximal value of 5.307 deg, found for L_2 = 0, to its minimal value of 0 deg, obtained for parallel tracks [8].

As illustrated in Fig. 2, the start position of the double-cone was empirically adopted at a distance L_S = 60 mm [6]. In this way, the initial span between the points of contact with rails becomes sufficiently large to achieve stable commencing conditions of the rolling motion, even for small values of L_2.

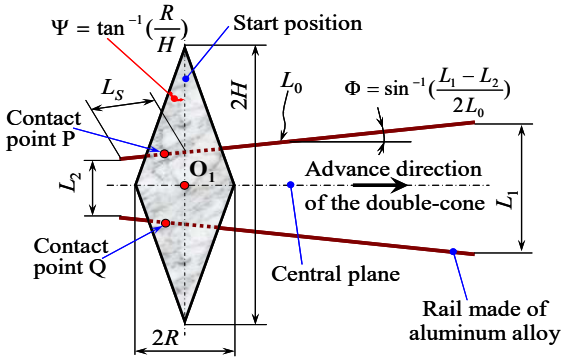

Fig. 2 Schematic view of the metallic or wooden double-cone, rolling on the V-shaped horizontal rails, made of aluminum alloy

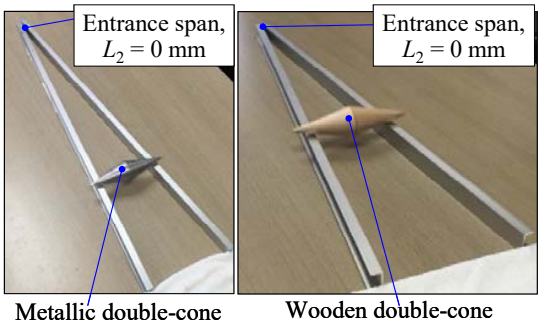

Fig. 3 Photographs of the metallic and wooden double-cones for an entrance span of L_2 = 0 mm

The following experimental procedure was adopted:

1) As shown in Fig. 2, rails made of A5052 aluminum alloy are positioned on a horizontal experimental table, with nil angle of inclination (0 ± 0.3 deg). Note that the radius of the double-cone cannot exceed the height of the rails ($R \leq H_0$). Exit span, which has to satisfy the condition $L_1 \leq 2H$, is fixed to a certain desired value, e.g., L_1 = 185 mm, in these particular tests.
2) Entrance span L_2, which has to satisfy the condition $L_2 \leq L_1$, is adjusted to a desired value (see Table II).
3) To avoid the supplying of input kinetic energy into the system, the double-cone is carefully placed on the rails at the start position of L_S = 60 mm (see Fig. 2).

4) Double-cone starts to self-propel along the rails due to the initially gained potential energy, which is transformed into the kinetic energy, of rotation and translation (see Fig. 10).
5) In order to easily observe the movement of the double-cone along the rails, generatrix lines and circular symbols were marked on the conical surface (see Fig. 1). For each entrance span of the rails, movies were shot from a convenient position near to the exit region of the tracks.

In the same time, the total traveling time T of the double-cone was measured by using a stopwatch. In order to achieve theoretical predictions with a relative error smaller than 5%, the reference experimental results should be quite accurately obtained. For this reason, three tests were carried-out for each experimental configuration, and the results were averaged.

6) Number of rotations, the variable period of rotation, and the total travelling times of the double-cones were determined as described in detail by [8].

III. Experimental Results and Their Significance

Number of rotations n, total traveling time T measured by using a stopwatch, and total traveling time T_m calculated from the recorded movies of the metallic and wooden double-cones are shown in Table II. Increase of the total traveling time and number of rotations of the double-cone can be observed at augmentation of the entrance span of the rails.

Relative difference between the total traveling time given by the stopwatch and the total traveling time determined from the slow-motion analysis of the recorded movies was found to be smaller than 5 %. Hence, it seems that the total traveling time of the double-cone was measured quite precisely.

However, rather large difference was unexpectedly obtained between the numbers of rotations n for the metallic and wooden double-cones. This result is unexpected, since the kinematical model [8] predicts the same number of rotations n_t, regardless the material used for the double-cone fabrication (Table II).

Results shown in the second column of Table II are obtained by starting from the following general expression of the total number of rotations n_t [8]:

$$n_t = -\frac{1}{2\pi \tan\alpha}\ln\left[1-\frac{(L_0-L_S)}{r_0}\sin\Phi\tan\Psi\right] \qquad (1)$$

Then, by substituting in (1) the opening angle Φ of the rails, the apex angle Ψ of the cone, the contact radius r_0 at the start position of the double-cone on the rails (see Fig. 10):

$$r_0 = \frac{R-0.5L_2\tan\Psi-L_S\sin\Phi\tan\Psi}{\cos^2\alpha}, \qquad (2)$$

and the angle $\alpha = \sin^{-1}(\tan\Psi\cdot\tan\Phi)$ of the trajectory of the mass center (see Figs. 9 and 10):

$$\alpha = \sin^{-1}\left[\frac{R}{H}\frac{L_1-L_2}{\sqrt{4L_0^2-(L_1-L_2)^2}}\right] \qquad (3)$$

the following expression, particularized for the ideal conical geometry with sharp tips, was derived as [8]:

$$n_t = -\frac{1}{2\pi\tan\alpha}\ln\left\{1-\frac{(L_0-L_S)(L_1-L_2)\cos^2\alpha}{2HL_0-[L_2L_0+(L_1-L_2)L_S]}\right\} \qquad (4)$$

Note that (1) was obtained from a kinematical model, in which the points of contact P and Q (Fig. 2), between the double-cone and rails, move on the conical surface along a three-dimensional logarithmic spiral. Besides, (1) was derived under the so-called "no-slip" or "pure rolling" condition, i.e. under the hypothesis that the distance $L_0 - L_S$ traveled by the contact point on the straight rail, equals the distance traveled by the same contact point along the logarithmic spiral trajectory.

Theoretical number of rotations n_t predicted by (4) together with (3) depends only on the geometrical parameters associated to the double-cone (R, H), and to the rails (L_0, L_1, L_2, and L_S). Hence, (4) predicts the same number of rotations n_t, regardless the material used for the double-cone fabrication. Although (4) gives results with a maximal relative error smaller than 11 %, for the metallic cone, the error increases up to 38 %, for the wooden cone (see Table II). In order to reduce the discrepancy between the theoretical and experimental results, an improved model is proposed in section IV, by including the influence of truncation of the conical tips.

As already stressed, the double-cone is unable to self-propel along parallel rails. Theoretical model reliably predicts such behavior, since by imposing the condition $L_2 = L_1$, one obtains from (4) a nil number of rotations, i.e., $n_t = \ln(1) = 0$.

TABLE II
Variation of the Number of Rotations, Total Traveling Time Measured by Using a Stopwatch, and Total Traveling Time Determined through the Slow-Motion Processing of the Recorded Movies, for the Metallic and Wooden Double-Cones

L_2	n_t	Metallic double-cone			Wooden double-cone		
[mm]	[-]	n [-]	T [s]	T_m [s]	n [-]	T [s]	T_m [s]
0	17.31	16.5	3.94	3.91	14.0	4.39	4.22
10	17.95	17.0	4.27	4.13	15.0	4.48	4.40
20	18.64	18.2	4.49	4.42	15.5	4.46	4.20
30	19.39	18.5	4.66	4.44	16.0	4.82	4.66
40	20.21	20.0	4.93	4.94	16.3	4.90	4.80
50	21.12	20.5	5.20	5.10	17.0	5.24	5.18
60	22.13	21.0	5.51	5.34	18.0	5.62	5.51
70	23.25	22.0	5.90	5.81	18.5	6.00	5.90
80	24.51	23.0	6.30	6.28	19.5	6.34	6.16
90	25.95	24.0	6.91	6.75	20.5	6.89	6.76
100	27.60	25.5	7.48	7.34	21.5	7.45	7.36
110	29.52	27.5	8.48	8.30	22.5	8.02	7.75
120	31.79	29.3	9.45	9.38	24.0	9.01	8.90
130	34.53	31.7	10.82	10.58	25.5	10.50	10.02
140	37.91	34.2	12.98	12.87	27.5	12.44	12.10
150	42.23	38.0	16.30	15.88	---	---	---

IV. Model Improvement by Considering the Effect of Truncation of the Conical Tips

As mentioned in section II, the actual manufactured cones are slightly truncated, to avoid injuries by the needle-like tips. Thus, Fig. 4 presents the geometry of the actually fabricated

cones, and Table III illustrates the corrected physical properties, relative to those shown by Table I, for the idealized cones.

Mass values remain unchanged, since they are not calculated, but measured for the actually fabricated double-cones, by using a digital balance. On the other hand, the moment of inertia I_t of the truncated cone has to be accurately recalculated as:

$$I_t = 0.3mR^2[1-(R^*/R)^5]/[1-(R^*/R)^3] \quad (5)$$

However, for the double-cones used in this work, insignificant change in the values of the moment of inertia was observed (i.e., $I_t \cong I$ as can be seen from Tables I and III).

Thus, main effect of truncation is the slight reduction in the apex angle, from the ideal value of $\Psi = \tan^{-1}(R/H) = 14.036$ deg (Table I), to values of $\Psi = \tan^{-1}[(R-R^*)/H] = 13.766$ deg, for the metallic cone, and 13.016 deg, for the wooden cone (Table III). Such angular change seems negligible, but due to the strong nonlinear effects induced by the logarithmic and trigonometric functions, it is responsible for the considerable alteration of the computed number of rotations.

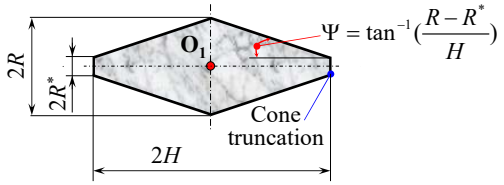

Fig. 4 Geometry of the actual double-cones, having truncated tips

TABLE III
REAL OR CORRECTED PHYSICAL PROPERTIES OF THE TESTED DOUBLE-CONES MADE OF CARBON STEEL AND WOOD

Property of the double-cone	Metallic	Wooden
Truncation diameter, $2R^*$ [mm]	1	4
Total height (length), $2H$ [mm]	200	199
Apex angle, Ψ [deg]	13.766	13.016
Moment of inertia, I_t [kg·mm^2]	197.0641	20.6730

Thus, by substituting the corrected apex angle in the model, one finds the revised contact radius r_0 at the start position of the double-cone on the rails:

$$r_0 = \frac{R}{\cos^2\alpha}\{1-[\frac{L_2}{2H}+\frac{(L_1-L_2)L_S}{2HL_0}](1-\frac{R^*}{R})\} \quad (6)$$

and the revised angle α of the trajectory of the mass center:

$$\alpha = \sin^{-1}[\frac{R-R^*}{H}\frac{L_1-L_2}{\sqrt{4L_0^2-(L_1-L_2)^2}}] \quad (7)$$

Also, the substitution of (6) in (1) leads to the revised number of rotations n_{tr} for the truncated double-cone, as follows:

$$n_{tr} = -\frac{\ln\{1-\dfrac{(L_0-L_S)(L_1-L_2)(1-\frac{R^*}{R})\cos^2\alpha}{2HL_0-[L_2L_0+(L_1-L_2)L_S](1-\frac{R^*}{R})}\}}{2\pi\tan\alpha} \quad (8)$$

Note that, by imposing the condition $R^* = 0$ in (6)-(8) of the truncated double-cones, one regains (2)-(4) of the ideal double-cones with sharp tips. On the other hand, by imposing the condition $R^* = R$ in (8), i.e., the double-cone transforms into a cylinder, one obtains a nil number of rotations, i.e. $n_{tr} = \ln(1) = 0$. Thus, the cylinder is unable to self-propel along horizontal V-shaped rails, a result well-known in the literature [5], [6].

Figs. 5 and 6 present the variation of the number of rotations versus the entrance span of the rails for the wooden and the metallic double-cones, respectively. Solid lines illustrate the results given by (4) for the ideal cone with sharp tips, circular symbols present the experimental results, and rhombic symbols show the results given by (8) for the truncated cones. Compared to the experimental results, (8) produces quite good predictions, with a maximal relative error smaller than 5%, both for the metallic and wooden double-cones.

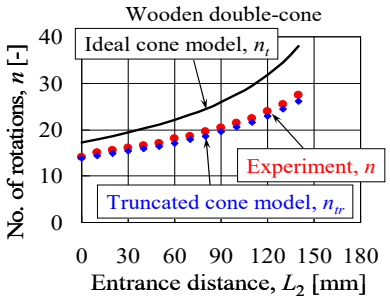

Fig. 5 Variation of the number of rotations versus the entrance span of the rails, for the wooden double-cone (Solid line: results for the ideal cone with sharp tips; circular symbols: experimental results; and rhombic symbols: results for the truncated cone)

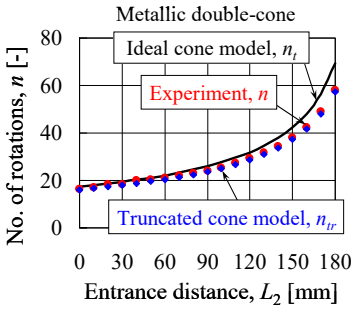

Fig. 6 Variation of the number of rotations versus the entrance span of the rails, for the metallic double-cone (Solid line: results for the ideal cone with sharp tips; circular symbols: experimental results; and rhombic symbols: results for the truncated cone)

In conclusion, improvement of the theoretical model was successfully achieved by taking into account the real geometry of the fabricated double-cones. It seems that not the material,

but the slight change in the apex angle, due to the truncation process, is responsible for the difference observed between the numbers of rotations for the metallic and wooden double-cones.

V. Law of Dynamics for the Translation Motion

Due to the geometrical and loading symmetry of the studied system relative to the O*x* axis (Fig. 7), the friction forces acting in the contact points P and Q during the movement of double-cone on the rails, are vectors occurring along the tracks, but opposing the advance direction of the double-cone [8]:

$$\begin{cases} \vec{F}_{f,P} = -F_f(\cos\Phi\vec{i} + \sin\Phi\vec{j}) \\ \vec{F}_{f,Q} = -F_f(\cos\Phi\vec{i} - \sin\Phi\vec{j}) \end{cases} \quad (9)$$

On the other hand, the reaction forces (see Figs. 8 and 9), acting in the same contact points P and Q, can be written as [8]:

$$\begin{cases} \vec{N}_P = N(\cos\Psi\sin\alpha\vec{i} - \sin\Psi\vec{j} + \cos\Psi\cos\alpha\vec{k}) \\ \vec{N}_Q = N(\cos\Psi\sin\alpha\vec{i} + \sin\Psi\vec{j} + \cos\Psi\cos\alpha\vec{k}) \end{cases} \quad (10)$$

Thus, Newton's Law of Dynamics, for the translation motion of the mass center O_1 of the double-cone, can be written as:

$$m\vec{a} = -mg\vec{k} + 2N\cos\Psi(\sin\alpha\vec{i} + \cos\alpha\vec{k}) - 2F_f\cos\Phi\vec{i} \quad (11)$$

which leads to the following scalar equations for accelerations along all three axes of the *xyz* system of coordinates:

$$\begin{cases} ma_x = 2N\cos\Psi\sin\alpha - 2F_f\cos\Phi \\ ma_y = 0 \\ ma_z = 2N\cos\Psi\cos\alpha - mg \end{cases} \quad (12)$$

As expected, due to the geometrical and loading symmetry of the studied system relative to the O*x* axis (see Figs. 7 and 8), the lateral acceleration becomes nil ($a_y = 0$); i.e., the mass center O_1 moves in the central vertical plane *x*O*z* (see Fig. 9).

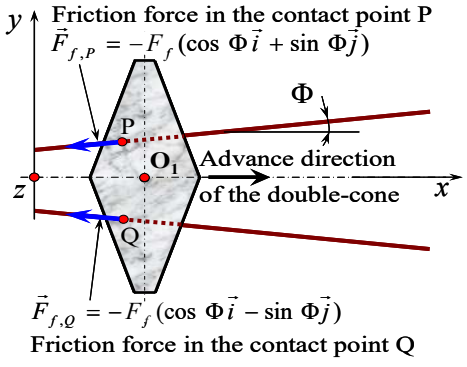

Fig. 7 Upper view of the contact between the double-cone and rails, showing the corresponding friction forces

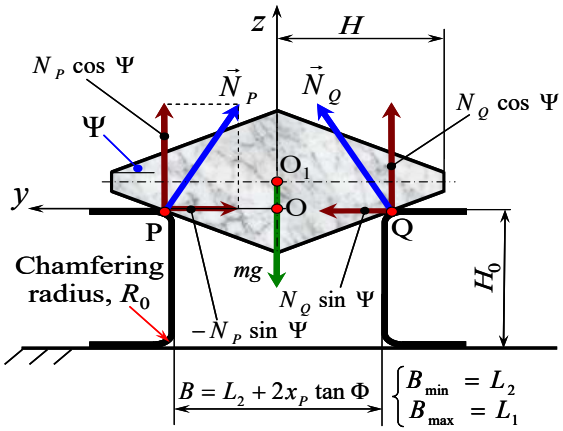

Fig. 8 Frontal view of the contact between the double-cone and rails, showing the corresponding normal and gravitational forces

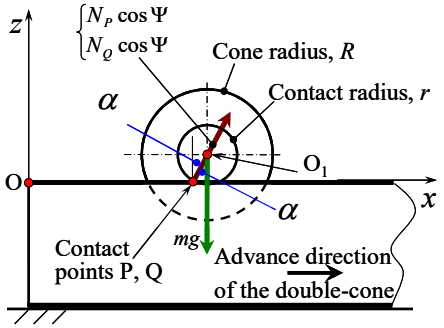

Fig. 9 Lateral view of the contact between the double-cone and rails, showing the corresponding normal and gravitational forces

Moduli *a*, *N*, and F_f of the acceleration vector, normal force, and friction force, can be determined from some kinematical conditions, which are depending on the actual regime of motion of the double-cone. Typically, three movement regimes can be encountered, as follows: pure sliding (slipping), pure rolling, and a combination of rolling and slipping [7], [10].

In order to establish the movement regime of double-cones, one rewrites (1) along the rails, as follows:

$$m\frac{a_x}{\cos\Phi} = 2N\frac{\cos\Psi}{\cos\Phi}\sin\alpha - 2F_f = 2N\mu_t - 2F_f \quad (13)$$

Term $2N\mu_t$ can be regarded as a traction force acting on the cone, and $\mu_t = \cos\Psi\sin\alpha/\cos\Phi$ as a traction coefficient.

Slipping commences if the traction force is larger than the static sliding friction force ($2N\mu_s$), and then, slipping is maintained if the traction force exceeds the dynamic sliding friction force ($2N\mu$).

For the ideal double-cones (Table I), the traction coefficient monotonically decreases from a value of 0.0226 for $L_2 = 0$, to a value of 0.0006 for $L_2 = 180$ mm. For the real truncated wooden (metallic) cone, the traction coefficient monotonically reduces from a value of 0.0210 (0.0222) for $L_2 = 0$, to a value of 0.0051 (0.0042) for $L_2 = 140$ mm (150 mm). Consequently, the traction

coefficient is much smaller than the static and dynamic sliding friction coefficients (0.3 and 0.2 for the wooden cone; 0.61 and 0.47 for the metallic cone, see Table I).

Accordingly, the assumption of "no-slip" or "pure rolling", used to derive the models (4) and (8), seems to be justified.

In order to clarify aspects concerning the trajectory, velocity and acceleration of the mass center, one firstly considers the relationship between the coordinates of the contact point P, and mass center O_1, as follows (see Fig. 9):

$$\begin{cases} x_{O_1} = x_P + r\sin\alpha \\ y_P = 0.5L_2 + x_P\tan\Phi \quad (y_{O_1} = 0) \\ z_{O_1} = r\cos\alpha \quad (z_P = 0) \end{cases} \tag{14}$$

where the instantaneous contact radius r can be written as [8]:

$$r = \frac{R - 0.5L_2\tan\Psi - x_{O_1}\sin\alpha}{\cos^2\alpha} \tag{15}$$

Concerning the trajectory of the mass center, by differentiating (14) and (15), one obtains the following relationship between the vertical and longitudinal coordinates of the point O_1:

$$\frac{dz_{O_1}}{dx_{O_1}} = \frac{dz_{O_1}}{dr}\frac{dr}{dx_{O_1}} = \cos\alpha\left(\frac{-\sin\alpha}{\cos^2\alpha}\right) = -\tan\alpha \tag{16}$$

This means that the mass center of the double-cone moves on a descending straight line that displays an inclination angle α relative to the horizontal line (Fig. 10). Such result agrees with the previously reported findings [6], [8].

Next, by differentiating against the time t the third equation of (14) and (15), one obtains:

$$V_{O_1,z} = \frac{dr}{dt}\cos\alpha \quad ; \quad \frac{dr}{dt} = -V_{O_1,x}\frac{\sin\alpha}{\cos^2\alpha} \tag{17}$$

which leads after some manipulations, to the following velocity components of the mass center:

$$\begin{cases} V_{O_1,x} = V\cos\alpha \\ V_{O_1,y} = 0 \\ V_{O_1,z} = -V\sin\alpha \end{cases} \quad ; \quad V = \sqrt{V_{O_1,x}^2 + V_{O_1,y}^2 + V_{O_1,z}^2} \tag{18}$$

Then, by differentiating (18) against the time t, one finds the acceleration components of the mass center, as follows:

$$\begin{cases} a_x = a\cos\alpha \\ a_y = 0 \\ a_z = -a\sin\alpha \end{cases} \quad ; \quad a = \sqrt{a_x^2 + a_y^2 + a_z^2} \tag{19}$$

As expected, the lateral velocity and acceleration of the mass center becomes nil, since the point O_1 moves in the central vertical plane xOz. Moreover, the velocity $\vec{V}$ and acceleration $\vec{a}$ are vectors perpendicular on the instantaneous contact radius, and consequently, they move on the same straight line as the point O_1 (see Fig. 10).

Thus, the gradual reduction of the contact radius leads to the height reduction Δz of the mass center of the double-cone. This causes a proportional decrease of the potential energy:

$$\Delta E_p = mg\Delta z = mg(r_0 - r)\cos\alpha \tag{20}$$

from an initial or input potential energy $E_{p,0} = mgr_0\cos\alpha$ (Fig. 10). Hence, such mechanism can be regarded as a gravitational motor, which transforms the initial or input potential energy into the kinetic energy, of rotation and translation. In order to fully determine the energy $E_{p,0}$ one needs the initial contact radius r_0, which for the truncated double-cones is given by (6).

Finally, by substituting (19) in (12), and retaining only the first and third equations, which contain the desired information, one obtains a set of two equations with three unknowns (the moduli a, N, and F_f), as follows:

$$\begin{cases} ma\cos\alpha = 2N\cos\Psi\sin\alpha - 2F_f\cos\Phi \\ -ma\sin\alpha = 2N\cos\Psi\cos\alpha - mg \end{cases} \tag{21}$$

In order to solve the problem, a third equation, obtained by applying the Law of Dynamics for the rotation movement of the double-cone, will be added in the next section.

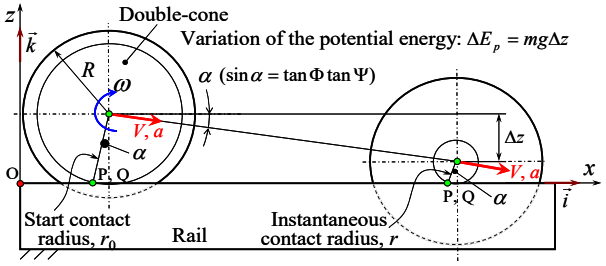

Fig. 10 Change in the contact radius, and implicitly, change in the height of the mass center due to the motion of the double-cone on rails

VI. Law of Dynamics for the Rotation Motion

First, in order to clarify the angular velocity ω of the rolling double-cone, it is useful to observe that the number of rotations N^* of the double-cone, at a certain instant t, can be expressed as:

$$N^*(t) = -\frac{1}{2\pi\tan\alpha}\ln\left[1 - \frac{S(t)}{r_0}\sin\Phi\tan\Psi\right] \tag{22}$$

where $S(t)$ is the instantaneous distance traveled by the contact point P along the straight rail, which can be calculated as:

$$S(t) = \frac{x_P(t) - x_P(t=0)}{\cos\Phi} \tag{23}$$

Combining the first equation of (14) and (15), one obtains

that the instantaneous contact radius r can be written as:

$$r(t) = R - 0.5L_2 \tan\Psi - x_P(t)\sin\alpha \quad (24)$$

which allows us to rewrite (23) as follows:

$$S(t) = \frac{r_0 - r(t)}{\sin\alpha\cos\Phi} = \frac{r_0 - r(t)}{\sin\Phi\tan\Psi} \quad (25)$$

By substituting (25) in (22), the number of rotations N^* of the double-cone, at a certain instant t, can be rewritten as:

$$N^*(t) = -\frac{1}{2\pi\tan\alpha}\ln[\frac{r(t)}{r_0}] \quad (26)$$

Then, the angular velocity ω can be derived as:

$$\omega = 2\pi\frac{dN^*}{dt} = -\frac{2\pi}{2\pi\tan\alpha}\frac{r_0}{r}\frac{1}{r_0}\frac{dr}{dt} = -\frac{dr/dt}{r\tan\alpha} \quad (27)$$

in which the derivative dr/dt can be substituted from the second equation of (17), combined with (18), as follows:

$$\frac{dr}{dt} = -V_{O_1,x}\frac{\sin\alpha}{\cos^2\alpha} = -V\tan\alpha \quad (28)$$

Finally, the angular velocity of the double-cone is found as:

$$\omega = V/r \quad (29)$$

This unexpectedly means that, the spinning speed ω (Fig. 10) is simply proportional to the velocity of the mass center O_1, and inversely proportional to the contact radius. Thus, although the double-cone has a variable contact radius, result (29) is similar to formulae obtained for objects of constant radius of contact, such as cylinders or spheres rolling on straight parallel tracks.

Next, in order to explain the self-propelling ability of the double-cone along the rails, the Law of Dynamics for rotation is applied relative to the PQ axis, determined by the contact points. Note that the normal forces N_P and N_Q, the friction forces $F_{f,P}$ and $F_{f,Q}$, and the component $mg\cos\alpha$ of the gravitational force are vectors passing through the PQ axis (Figs. 7-9). Hence, they are unable to cause revolution of the double-cone around this axis. Only the component $mg\sin\alpha$ of the gravitational force is able to cause clockwise rotation of the double-cone around the PQ axis (Fig. 9). Thus, the corresponding moment of revolution can be written as:

$$M_{t,P} = mgr\sin\alpha \quad (30)$$

Since the torque (30) is responsible for commencing the rolling of the double-cone along rails, it appears to be a traction torque.

For parallel rails ($L_2 = L_1$), the angles Φ and α become nil (see Fig. 2 and (7)). Hence, the traction torque (30) becomes zero, and as expected, the double-cone is unable to self-propel against such parallel tracks.

Equation describing the starting of the double-cone's rolling movement on the rails can be written as:

$$I_P\varepsilon_P = M_{t,P} \quad (31)$$

where ε_P is the angular acceleration, and I_P is the moment of inertia of the double-cone against the PQ axis (see also (5)):

$$I_P = I_t + mr^2 \cong I + mr^2 = m(r^2 + 0.3R^2) \quad (32)$$

Thus, the easiest way to achieve rotation of the double-cone is around its axis of symmetry. The higher moment of inertia (32) relative to the PQ axis implies that larger torque is needed to spin the double-cone around this axis. Substituting (32) in (31), one finds the expression of angular acceleration versus radius r:

$$\varepsilon_P = g\sin\alpha\frac{r}{r^2 + 0.3R^2} \quad (33)$$

Fig. 11 shows that the angular acceleration increases when the contact radius reduces from its initial (maximal) value r_0 to $0.548R$, and then decreases when r further reduces from $0.548R$ to the final (minimal) radius of contact r_f. Such behavior was confirmed by the films shot for the rolling double-cones.

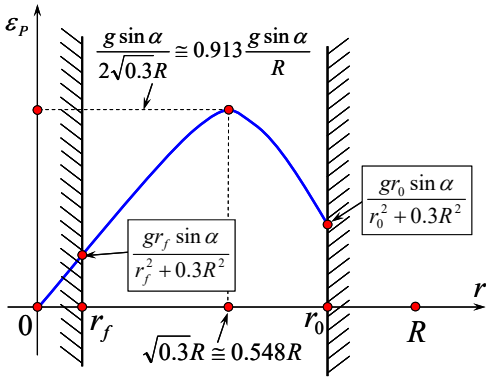

Fig. 11 Variation of the angular acceleration versus the contact radius

Note that, by substituting the final value of the longitudinal coordinate of the mass center $x_{O_1} = L_0\cos\Phi$ (see Figs. 2 and 7) in (15), the minimal contact radius can be found, as follows:

$$r_f = \frac{R}{\cos^2\alpha}[1 - \frac{L_1}{2H}(1 - \frac{R^*}{R})] \quad (34)$$

Adequate design of the gravitational motor is achieved if the minimal radius exceeds the truncation radius ($r_f \geq R^*$).

On the other hand, the Law of Dynamics for rotation can be applied relative to the axis of symmetry of the double-cone.

From this different point of view, the components $N_P \cos\Psi$ and $N_Q \cos\Psi$ of the normal forces, and also the gravitational force, are vectors passing through the axis of symmetry of the double-cone (see Fig. 8). Hence, they are unable to cause revolution of the double-cone around this axis. Moreover, the components $N_Q \sin\Psi$ and $-N_P \sin\Psi$ of the normal forces, and the lateral components $\pm F_f \sin\Phi$ of the friction forces, are vectors parallel to the axis of symmetry of the double-cone (see Figs. 7-9). Hence, they are also unable to produce revolution. Only the longitudinal components $2F_f \cos\Phi$ of the friction forces are able to cause clockwise rotation of the double-cone. Their corresponding moment of revolution can be written as:

$$M_{t,O_1} = 2F_f r \cos\Phi \cos\alpha \tag{35}$$

Since this traction torque is produced by the dynamic friction force, which occurs after the rolling process has commenced, it can be regarded as a torque responsible for the continuation of the previously started rolling movement of the double-cone along the rails. Thus, the torque $M_{t,P}$ appears to be the cause, and the torque M_{t,O_1} appears to be the effect. Also, the dynamic friction force F_f appears to be a desired force.

Next, one analyzes the ratio of the traction torques (35) and (30), which can be derived based on (21), as:

$$\frac{M_{t,O_1}}{M_{t,P}} = \frac{2F_f \cos\Phi}{mg\tan\alpha} = 1 - \frac{a}{g\sin\alpha} < 1 \tag{36}$$

Because the acceleration a of the mass center is positive, as expected, the rolling starting torque $M_{t,P}$ that is induced by the gravitational force is larger than the rolling continuation torque M_{t,O_1} that is produced by the dynamic friction force.

Since the continuation of the double-cone's rolling on the rails can be described by:

$$I\varepsilon = M_{t,O_1} \tag{37}$$

the angular acceleration ε of the mass center can be derived, after some manipulations of (35)-(37), as:

$$\varepsilon = (g\sin\alpha - a)\frac{r}{0.3R^2} \tag{38}$$

Condition of pure rolling of the double-cone can be imposed in two different ways. In the usual way, one imagines that the acceleration at the contact point P is nil, this leading to:

$$a_P = a - \varepsilon r = 0 \quad \Rightarrow \quad a = \varepsilon r \tag{39}$$

Nevertheless, the condition of pure rolling can be understood in a more intuitive manner, by imagining that the acceleration of the mass center equals the tangential acceleration produced by the rotation of the double-cone around the PQ axis, i.e.:

$$a = \varepsilon_P r = g\sin\alpha \frac{r^2}{r^2 + 0.3R^2} \tag{40}$$

VII. Results and Discussions

Both conditions (39) and (40), for the pure rolling movement of the double-cone, lead to the same results for the moduli of the normal force, friction force, and angular acceleration, as:

$$\begin{cases} 2N = mg\dfrac{1}{\cos\alpha\cos\Psi}\dfrac{r^2\cos^2\alpha + 0.3R^2}{r^2 + 0.3R^2} \\ 2F_f = mg\dfrac{\tan\alpha}{\cos\Phi}\dfrac{0.3R^2}{r^2 + 0.3R^2} \\ \varepsilon = \varepsilon_P = g\sin\alpha\dfrac{r}{r^2 + 0.3R^2} \end{cases} \tag{41}$$

Similarly to the sliding friction coefficient, based on (41), an equivalent friction coefficient can be defined, as:

$$\mu_e = \frac{F_f}{N} = \frac{0.3R^2\mu_t}{r^2\cos^2\alpha + 0.3R^2} \quad ; \quad \mu_t = \frac{\cos\Psi}{\cos\Phi}\sin\alpha \tag{42}$$

where μ_t is the traction coefficient, already defined in Section V (see (13)). As expected, the equivalent friction coefficient is smaller than the traction coefficient ($\mu_e < \mu_t$).

Note that the forces (41), accelerations (40)-(41), and the equivalent friction coefficient (42) can be regarded as functions of the instantaneous contact radius *r* of the double-cone.

Variation of the angular acceleration versus the radius of contact was already illustrated in Fig. 11. Additionally, from (41) and (42), one observes that, while the normal force, the friction force, and the equivalent friction coefficient monotonically increase, the acceleration monotonically decreases, when the contact radius reduces from its initial (maximal) value of r_0, to its final (minimal) value of r_f.

Fig. 12 presents the variation of the dimensionless angular acceleration $R\varepsilon / g$ versus the entrance span L_2 of the rails, for the initial and final radii of contact of the double-cone. One observes that the angular acceleration decreases against L_2, linearly at the final radius, and nonlinearly at the initial radius.

Fig. 13 shows the variation of the dimensionless acceleration a/g versus the entrance span L_2 of the rails, for the initial and final radii of contact of the double-cone. One observes that the acceleration monotonically decreases against L_2, both for the initial and final radii of contact. When the tracks become almost parallel (L_2 = 180 mm), both acceleration (Fig. 13) and angular acceleration (Fig. 12) approaches zero.

Fig. 14 illustrates the variation of the traction coefficient, and the variation of the equivalent friction coefficients versus the entrance span L_2 of the rails, for the initial and final radii of contact of the double-cone. As expected, traction coefficient is always larger than the friction coefficient, and the friction at r_f

is always higher than the friction at r_0. Note that the difference between traction coefficient and friction coefficient at r_f is very small. For this reason, the acceleration at r_f is closed to zero (Fig. 13). Traction coefficient and the friction coefficient calculated for r_f, decrease linearly against L_2. Conversely, the coefficient of friction calculated for r_0, increases up to a maximum reached at L_2 = 60 mm, and then, decreases nonlinearly versus L_2.

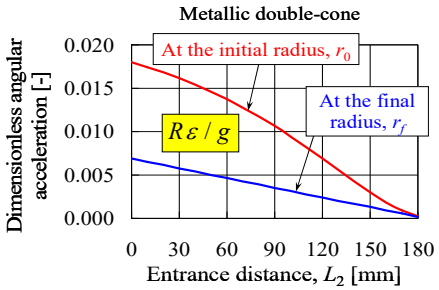

Fig. 12 Variation of the dimensionless angular acceleration versus the entrance span of the rails, for the initial and final radii of contact

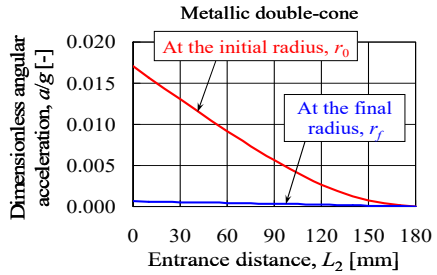

Fig. 13 Variation of the dimensionless acceleration versus the entrance span of the rails, for the initial and final radii of contact

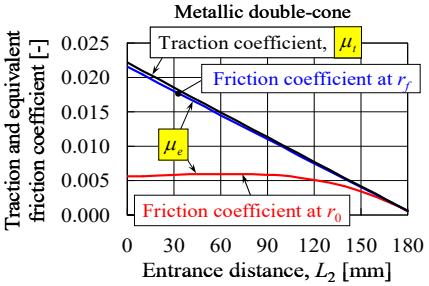

Fig. 14 Variation of the traction coefficient and equivalent friction coefficients versus the entrance span of the rails, for the initial and final radii of contact

To complete the Dynamic analysis of the gravitational motor, it is necessary to find the variation of the contact radius versus time. With this purpose, by differentiating (28) and substituting (40) in the resulting equation, the second derivative of the contact radius against time is obtained, as:

$$\frac{d^2r}{dt^2} = -a\tan\alpha = -g\sin\alpha\tan\alpha\frac{r^2}{r^2+0.3R^2} \tag{43}$$

Second order differential (43) is non-homogeneous due to the right-side $r^2/(r^2+0.3R^2)$ term. However, it can be solved in a first approximation, by developing in a Taylor series around r_0 the non-homogeneous term, and by retaining only the first, constant term. In such conditions, (43) can be rewritten as:

$$\frac{d^2r}{dt^2} = -g\sin\alpha\tan\alpha\frac{r_0^2}{r_0^2+0.3R^2} \tag{44}$$

By integrating (44) twice against the time, and by imposing the following boundary conditions:

$$r(t=0)=r_0 \quad ; \quad \frac{dr}{dt}(t=0) = -\tan\alpha\cdot V(t=0) = 0 \tag{45}$$

one finds the variation of the contact radius versus time, in a first approximation, as:

$$r(t) = r_0 - \frac{g}{2}\sin\alpha\tan\alpha\frac{r_0^2t^2}{r_0^2+0.3R^2} \tag{46}$$

Total travelling time T of the double-cone can be determined from the condition:

$$r(t=T) = r_f \tag{47}$$

which leads to:

$$T = \sqrt{\frac{2(r_0-r_f)}{g\sin\alpha\tan\alpha}\frac{r_0^2+0.3R^2}{r_0^2}} \tag{48}$$

Figs. 15 and 16 illustrate the variation of the total traveling time of the double-cone versus the entrance span of the rails, for the wooden and metallic cones, respectively. On these graphs, the solid red lines present the theoretical results, obtained in a first approximation by using (48). Circular symbols denote the data obtained during the rolling experiments.

One observes that the maximal relative difference between the theoretical and experimental results is smaller than 18 %, although the nonlinear term of (43) is reduced to a constant.

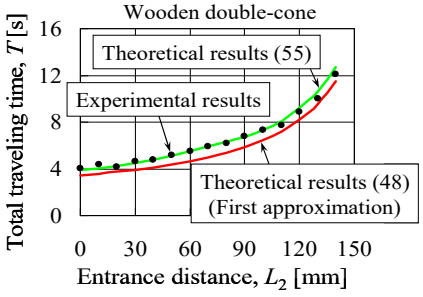

Fig. 15 Variation of the total traveling time versus the entrance span of the rails, for the wooden double-cone (red solid line: theoretical results predicted by (48); circular symbols: experimental results; and, green solid line: theoretical results predicted by (55))

Accuracy augmentation of the theoretical predictions can be achieved by reintegrating the differential equation (43), where the non-homogeneous term is better approximated, by substituting (46) for the contact radius. In such circumstances, (43) can be rewritten as:

$$\frac{d^2r}{dt^2} = -2r_0\Delta(1+\Sigma)\frac{(1-\Delta t^2)^2}{(1-\Delta t^2)^2+\Sigma} \tag{49}$$

where the parameters Δ and Σ are defined by:

$$\Delta = \frac{g}{r_0}\frac{\sin\alpha\tan\alpha}{2(1+\Sigma)} \quad ; \quad \Sigma = 0.3(\frac{R}{r_0})^2 \tag{50}$$

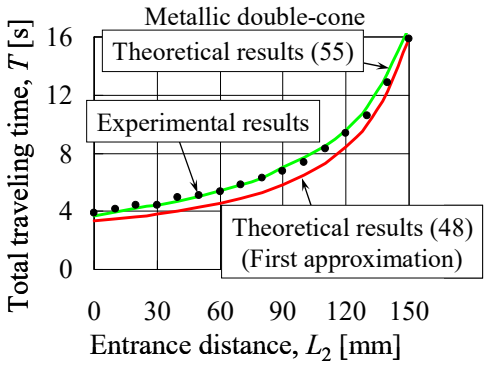

Fig. 16 Variation of the total traveling time versus the entrance span of the rails, for the metallic double-cone (red solid line: theoretical results predicted by (48); circular symbols: experimental results; and green solid line: theoretical results predicted by (55))

Then, by integrating (49) twice against the time, under the same boundary conditions (45), one obtains the variation of the contact radius versus time, in presumably, a more accurate second approximation, as:

$$\begin{aligned} r(t) &= r_0 - \frac{gt^2}{2}\sin\alpha\tan\alpha + \\ &+ \frac{\Sigma t}{2}\sqrt{r_0 g\sin\alpha\tan\alpha}\times[f_1(\Delta,\Sigma,t)+f_2(\Delta,\Sigma,t)] + \\ &+ \frac{r_0}{2}(1+\Sigma)\sqrt{\Sigma}\times[f_3(\Delta,\Sigma,t)-\tan^{-1}\frac{1-\Sigma}{2\sqrt{\Sigma}}] \end{aligned} \tag{51}$$

where functions f_1, f_2, f_3 are defined in the following manner.

Function $f_1(\Delta,\Sigma,t)$

$$f_1(\Delta,\Sigma,t) = \frac{\ln\sqrt{\frac{\Delta t^2 + t\sqrt{2\Delta(\sqrt{1+\Sigma}+1)}+\sqrt{1+\Sigma}}{\Delta t^2 - t\sqrt{2\Delta(\sqrt{1+\Sigma}+1)}+\sqrt{1+\Sigma}}}}{\sqrt{\sqrt{1+\Sigma}+1}} \tag{52}$$

Function $f_2(\Delta,\Sigma,t)$

$$f_2(\Delta,\Sigma,t) = \frac{\tan^{-1}\frac{t\sqrt{2\Delta(\sqrt{1+\Sigma}-1)}}{\sqrt{1+\Sigma}-\Delta t^2}}{\sqrt{\sqrt{1+\Sigma}-1}} \tag{53}$$

Function $f_3(\Delta,\Sigma,t)$

$$f_3(\Delta,\Sigma,t) = \tan^{-1}\frac{(1-\Delta t^2)^2-\Sigma}{2(1-\Delta t^2)\sqrt{\Sigma}} \tag{54}$$

Again, the total traveling time T of the double-cone can be determined by imposing the condition (47), which leads to the following transcendent equation, to be solved for T:

$$\begin{aligned} r_f &= r_0 - \frac{gT^2}{2}\sin\alpha\tan\alpha + \\ &+ \frac{\Sigma T}{2}\sqrt{r_0 g\sin\alpha\tan\alpha}\times[f_1(\Delta,\Sigma,T)+f_2(\Delta,\Sigma,T)] + \\ &+ \frac{r_0}{2}(1+\Sigma)\sqrt{\Sigma}\times[f_3(\Delta,\Sigma,T)-\tan^{-1}\frac{1-\Sigma}{2\sqrt{\Sigma}}] \end{aligned} \tag{55}$$

Results obtained by using (55) are shown in solid green lines on Figs. 15 and 16, for the wooden and metallic double-cones. Maximal relative difference, between the results predicted by (55) and the experimental results, is smaller than to 5.9 %. Thus, as expected, (55) offers more accurate predictions than (48). However, since there is no analytical closed solution for (55), the transcendent equation has to be numerically solved.

VIII. Conclusions

In this paper, frictional effects on the dynamics of truncated metallic and wooden double-cones, able to self-propel on straight tracks that are placed on a horizontal table to form a V letter, were evaluated. From the experimental and theoretical analysis of this conical gravitational motor, the following conclusions can be drawn:

1) Total number of rotations depends only on the geometrical parameters associated to the double-cone and rails, i.e. the base circle radius, truncation radius, and height of the cone, the length, exit span and entrance span of the rails, as well as the start position of the cone on the tracks.
2) An improved theoretical model was achieved by considering the real geometry of the double-cone, i.e. by including the effect of truncation of the conical tips. Based on such model, the number of rotations of the cone was predicted quite accurately, i.e. with a relative error lower than 5%.
3) Main effect of conical truncation was found to be a slight change in the apex angle of the cones. Although, such angular change seems negligible at a first glance, due to the strong nonlinear effects induced by the trigonometric and logarithmic functions, it produces considerable change of the calculated number of rotations.
4) Traction coefficient was found to be much smaller than the static and dynamic sliding friction coefficients. This

feature justified the assumption of "no-slip" or "pure rolling", used to derive the theoretical model.

5) Augmentation of the total traveling time and number of rotations of the double-cone was observed at enlargement of the entrance span of the rails. However, double-cone was unable to self-propel along parallel tracks. Proposed model reliably predicted such behavior, and also the well-known fact that a cylinder cannot self-propel on horizontal V-shaped rails.
6) Although the double-cone has a variable contact radius, its spinning speed has found to be proportional to the velocity of the mass center, and inversely proportional to the contact radius. Unexpectedly, such result is similar to formulae obtained for objects of constant radius of contact, such as cylinders and spheres rolling on straight parallel tracks.
7) Angular acceleration increased up to a point of maximum and then decreased, when the contact radius was reduced, from its initial (maximal) value, to its final (minimal) value.
8) While the normal force, friction force, and the equivalent friction coefficient monotonically increased, the acceleration monotonically decreased when the contact radius was reduced, from its initial value, to its final value.
9) Dimensionless angular and translational accelerations of the mass center monotonically decreased versus the entrance span of the rails, linearly at the final contact radius, and nonlinearly at the initial contact radius. When tracks became parallel, both accelerations approached zero.
10) Equivalent friction coefficient was smaller than traction coefficient. Friction estimated at the final radius of contact was higher than friction determined at the initial radius of contact.
11) Traction coefficient, and friction coefficient, calculated at the final radius of contact, decreased linearly versus the entrance span of the rails. On the other hand, friction coefficient estimated at the initial radius of contact, increased slightly up to a maximal value, and then, decreased nonlinearly versus the entrance span of the rails.
12) Total traveling time of the double-cone was computed, in a first approximation, quite easily but somewhat imprecisely, by employing an analytical expression. As alternative, to obtain more accurate predictions, a transcendent equation to be solved numerically for the total traveling time, was suggested.

Acknowledgment

Support from Mr. H. OHTSUKA from the Manufacturing Center, affiliated to the Fukuoka Institute of Technology, Japan is acknowledged.

References

[1] http://alltechscience.com/physics-nerds-info/2015-inventions-amazing-automated-inventions-of-the-world/
[2] http://www.leonardodavincisinventions.com/mechanical-inventions/leonardo-perpetual-motion-machine/
[3] D. Gardner, and M.E. Hiscox, *Mechanical Appliances and Novelties of Construction*. London: Norman W. Henley Publ. Co., 1927, p. 121.
[4] S. Iwnicki, *Handbook of Railway Vehicle Dynamics*. New York: CRC Press, Taylor & Francis, 2006, pp. 6–8.
[5] A. A. Gallitto, and E. Fiordilino, "The Double Cone: A Mechanical Paradox or a Geometrical Constraint?," *Physics Education*, 46, pp. 682–684, 2011.
[6] S.C. Gandhi, and C.J. Efthimiou, "The Ascending Double-Cone: A Closer Look at a Familiar Demonstration," *European Journal of Physics*, 26, pp. 681–697, 2005.
[7] A. Domenech, T. Domenech, and J. Cebrian, "Introduction to the Study of Rolling Friction," *American Journal of Physics*, 55(3), pp. 231–235, 1987.
[8] B. Suciu, "On the Kinematics of a Double-Cone Gravitational Motor," *International Journal of Science and Engineering Investigations*, 5(53), pp. 1–7, 2016.
[9] U. Olofsson, and R. Lewis, *Tribology of the Wheel-Rail Contact*. New York: Taylor & Francis, 2012, pp. 121–141.
[10] G.W. Stachowiak, and A.W. Batchelor, *Engineering Tribology*. 3rd ed., London: Elsevier, 2005, pp. 287–362, 461–499.
[11] A. Kapoor, D.I. Fletcher, F. Schmid, K.J. Sawley, and M. Ishida, *Tribology of Rail Transport*. New York: CRC Press, 2001, pp. 161–202.

Barenten Suciu was born on July 9, 1967. He received Dr. Eng. Degrees in the field of Mech. Eng. from the Polytechnic University of Bucharest, in 1997, and from the Kobe University, in 2003. He is working as Professor at the Department of Intelligent Mech. Eng., Fukuoka Institute of Technology. He is also entrusted with the function of Director of the Electronics Research Institute, affiliated to the Fukuoka Institute of Technology. He is member of JSME and JSAE. His major field of study is the tribological and dynamical design of various machine elements.